Reconciling modelled and observed $\Delta^{17}O(NO_3^-)$ in Beijing winter haze with heterogeneous chlorine chemistry

Zhongyi Zhang[1], Zhuang Jiang[1], Tao Zhou[1], Lei Geng[1,2]*

[1]Deep Space Exploration Laboratory/School of Earth and Space Sciences, University of Science and Technology of China, Hefei, Anhui, China

[2]CAS Center for Excellence in Comparative Planetology, University of Science and Technology of China, Hefei 230026, Anhui, China.

*Correspondence to: Lei Geng (genglei@ustc.edu.cn)

Abstract

The air quality in Chinese megacities has been improved as indicated by large decreases in fine particulate matter ($PM_{2.5}$) due to remarkable decreases in key precursors (e.g., SO_2, NO_x) after the implementation of strict mitigation strategies. However, nitrate concentrations in $PM_{2.5}$ (p-NO_3^-) have not decreased and mass fractions of p-NO_3^- in $PM_{2.5}$ have increased, especially during wintertime haze events. Discerning chemical mechanisms leading to nitrate growth during haze events is critical to implement effective mitigation policies. Chemical transport models incorporating oxygen isotope anomaly of nitrate ($\Delta^{17}O(NO_3^-)$) have been widely used to investigate nitrate formation mechanisms, showing general consensus on the modelled and observed $\Delta^{17}O(NO_3^-)$. However, under Beijing haze days, the same model tends to underestimate observed $\Delta^{17}O(NO_3^-)$. Here we compiled reported $\Delta^{17}O(NO_3^-)$ data in Beijing haze along with relevant observational parameters (e.g., OH total reactivity, peroxyl radical concentrations), tested assumptions on $\Delta^{17}O$ of key precursors (e.g., OH and NO_2), re-calculated $\Delta^{17}O(NO_3^-)$ and compared with observations. Our results indicate that considering heterogeneous N_2O_5 reactions on Cl^--containing aerosols with a $ClNO_2$ yield of ~ 0.75 can explain the observed high $\Delta^{17}O(NO_3^-)$. According to the $\Delta^{17}O(NO_3^-)$ data, this heterogeneous N_2O_5 + Cl^- chemistry can explain $\sim 60\%$ of nighttime nitrate production and makes daytime and nocturnal pathways equally important in winter Beijing haze. Meanwhile, the high yield of $ClNO_2$ means that on the following day the subsequent photolysis of $ClNO_2$ would enhance atmospheric oxidation capacity and promote haze pollution, highlighting the critical role of reactive chlorine chemistry in air pollution/chemistry in inland cities.

Plain language summary

$\Delta^{17}O(NO_3^-)$ has been proposed to be useful in assessing the nitrate formation mechanisms. However, the GEOS-Chem model persistently underestimates the observed $\Delta^{17}O(NO_3^-)$ during extreme haze periods in urban Beijing, implying an unknown or misunderstood NO_x chemistry characterized by high $\Delta^{17}O$ signatures. Here, we aim to reconcile the discrepancy to better understand the nitrate formation mechanisms in winter haze in Beijing. To this end, we re-assess the isotopic signatures of key precursors relating to the NO_x chemistry constrained by atmospheric

chemistry parameters (e.g., OH and OH reactivity, HO_2 and RO_2). We find that 1) steady-state OH radical should bear positive $\Delta^{17}O$ values but are unable to reconcile the gap between the observed and modelled $\Delta^{17}O(NO_3^-)$; 2) $ClNO_2$ production is efficient under typical haze conditions in urban Beijing, which is able to explain the gap between the model predicted and observed $\Delta^{17}O(NO_3^-)$. The photolysis of $ClNO_2$ has significant effects on atmospheric oxidative capacity and aerosol pollution. Although halogen chemistry is prevailing in the marine boundary layer, our results highlight the important roles of halogen chemistry in nitrate pollution which should be comprehensively incorporated into the air quality models and field observational research to better understand the atmospheric chemistry in urban air.

Key Points:

- Heterogeneous N_2O_5 + Cl⁻ chemistry is important for nitrate production in winter Beijing haze.

- A $ClNO_2$ yield of 0.75 from the heterogeneous N_2O_5 + Cl⁻ chemistry can explain both the observed high $\Delta^{17}O(NO_3^-)$ and $ClNO_2$ concentration.

- Diurnal sampling and subsequent data interpretation need to consider the differences in the surface and the residual layers.

1. Introduction

Since 2013, air quality in most regions of China has steadily improved following the implementation of a series of clean air policies and measures, e.g., "Action Plan for Air Pollution Prevention and Control" [*Q Zhang et al.*, 2019]. Substantial reductions in atmospheric pollutants have been observed across China over the past decade, particularly in the North China Plain (NCP) [*Cheng et al.*, 2019; *Q Zhang et al.*, 2019]. In particular, from 2013 to 2017, emissions of SO_2 and NO_x ($NO + NO_2$) in the NCP have decreased by approximately 59.5% and 22.9%, respectively, leading to significant declines in the total mass of fine particulate matter ($PM_{2.5}$) and sulfate concentrations [*Cheng et al.*, 2019; *Zhou et al.*, 2019]. However, the concentration of nitrate in $PM_{2.5}$ (particulate nitrate, p-NO_3^-) has only decreased in summer but with little changes in winter [*Xie et al.*, 2022; *Zhai et al.*, 2021], making high loadings of p-NO_3^- a principal cause of winter haze pollution in recent years [*Fu et al.*, 2020]. A similar non-linear response of nitrate production to NO_x emission reductions has also been observed in Western Europe and the Eastern United States [*Shah et al.*, 2018; *Tørseth et al.*, 2012]. Abatement of p-NO_3^- is now an increasing priority to reduce $PM_{2.5}$ pollution in China.

The decoupling between NO_x emission reduction and p-NO_3^- concentration could be attributed to various factors, e.g., varying nitric acid (HNO_3) formation mechanisms, HNO_3 gas-particle partitioning, deposition mechanisms of atmospheric nitrate, etc. [*Fu et al.*, 2020; *Seinfeld and Pandis*, 2016; *Z Zhang et al.*, 2020]. Typically, the gas-particle partitioning of HNO_3 is influenced by temperature, relative humidity, and particle acidity [*Guo et al.*, 2017]. In the urban environment of China during winter, where gaseous ammonia (NH_3) is abundant and temperature is low, atmospheric nitrate is assumed to primarily exist in the particle phase [*M Liu et al.*, 2017; *Zhai et al.*, 2021]. Moreover, because particulate nitrate deposition velocity is about 5-15 times slower than gaseous nitrate [*Zhai et al.*, 2021], the deposition of particle phase nitrate dominates the lifetime of total atmospheric nitrate and even a small alteration of the gas-particle partition ratio would significantly impact the retention of atmospheric nitrate. In the NCP region, the weak response of p-NO_3^- to NO_x emission reduction is probably in part caused by increases in particulate nitrate fraction in total atmospheric nitrate (90% in 2013 to 98% in 2017), which

extends the lifetime of total atmospheric nitrate against deposition [*Zhai et al.*, 2021]. A similar subdued response of p-NO_3^- to NO_x emission reduction controlled by the gas-particle partition process over the Eastern United States has been investigated by Shah et al., 2018 [*Shah et al.*, 2018]. They observed an increase in particulate nitrate fraction relative to total atmospheric nitrate from 29% in 2007 to 44% in 2015 due to decreases in particle acidity [*Shah et al.*, 2018]. The subdued response of p-NO_3^- to NO_x emission reduction can also be caused by enhanced conversion efficiency of NO_x to HNO_3 [*Fu et al.*, 2020; *Zang et al.*, 2022]. For instance, a modeling study by Fu et al. 2020 suggested that the mixing ratio of O_3 and OH increased by approximately 30% from 2010 to 2017 in the NCP, and this led to an enhanced conversion efficiency of NO_x to HNO_3 by 38.7% [*Fu et al.*, 2020], partially offsetting the effect of decreasing NO_x emission on nitrate production. Field observations have also indicated that in NCP the wintertime atmospheric oxidation capacity is unexceptionally high, characterized by a high OH oxidation rate and ozone production rate [*Lu et al.*, 2019]. This increased atmospheric oxidation capacity, which may be relevant to pollution mitigation strategies, counteracts the effect of reduced NO_x emissions on nitrate production [*Lu et al.*, 2019; *Leung et al.*, 2020; *M Liu et al.*, 2022]. Overall, in order to better understand the non-linear response of p-NO_3^- to NO_x emission decline, a thoughtful understanding of the chemical mechanisms driving the conversion of NO_x to nitrate is important.

Conventionally, the major formation pathways of atmospheric nitrate in inland cities include (1) the oxidation of NO_2 by OH radical in the daytime and (2) the heterogeneous uptake of N_2O_5 on wet aerosol at night. There is an increasing body of investigations on nitrate formation mechanisms across China, especially during winter haze events over the NCP region [*Chen et al.*, 2016; *Fu et al.*, 2020; *Su et al.*, 2017; *H Wang et al.*, 2022; *Xie et al.*, 2022] (and references therein). However, the dominant formation pathway leading to the explosive growth of pNO_3^- is still a subject of debate [*Chan et al.*, 2021; *H Wang et al.*, 2022; *Xie et al.*, 2022]. A variety of chemical transport models (CTMs) have been used to investigate the sources and formations of p-NO_3^- [*Chan et al.*, 2021; *Seinfeld and Pandis*, 2016; *Su et al.*, 2017; *Zhao et al.*, 2023; *Xie et al.*, 2022]. These model results are uncertain due to challenges in accurately representing the hydrolysis of N_2O_5 on aerosol [*H Wang et al.*, 2020; *Yang et al.*, 2022; *Yu et al.*, 2020; *Xie et al.*,

2022] and most models struggle to properly reproduce the observed concentrations of oxidants such as OH and HO_2/RO_2 radicals [*Slater et al.*, 2020]. By incorporating updated N_2O_5 heterogeneous chemistry (i.e., N_2O_5 heterogeneous uptake coefficient on aerosols, $ClNO_2$ yield) and reactive nitrogen chemistry, Fu et al., 2020 found that the N_2O_5 heterogeneous hydrolysis and the OH + NO_2 reaction contribute 43% and 44% of nitrate production within the planetary boundary layer, respectively [*Fu et al.*, 2020]. In comparison, by direct measurement of atmospheric radicals and relevant parameters (i.e., OH, N_2O_5), some observational constrained box models calculated that OH oxidation reaction is much more important than N_2O_5 hydrolysis in wintertime nitrate formation [*X Chen et al.*, 2020; *Slater et al.*, 2020; *Tan et al.*, 2018]. For example, a study based on ground and tall-tower field observations suggested that the gas-phase OH oxidation pathway dominates wintertime nitrate production in urban Beijing (average of 74%) [*X Chen et al.*, 2020].

Nitrate oxygen isotope signatures, particularly $\Delta^{17}O$ ($\Delta^{17}O = \delta^{17}O - 0.52*\delta^{18}O$) have been widely used to quantify nitrate formation pathways [*Alexander*, 2009; *Geng et al.*, 2017; *Hastings*, 2004; *He et al.*, 2018; *Michalski et al.*, 2003; *Morin et al.*, 2008; *Savarino et al.*, 2016]. Unlike conventional methods, this isotope tool provides direct constraints on the chemical fluxes of individual reactions contributing to nitrate formation [*Geng et al.*, 2017; *Michalski et al.*, 2003; *Morin et al.*, 2008]. Theoretically, nitrate $\Delta^{17}O$ signature ($\Delta^{17}O(NO_3^-)$) generated from daytime OH + NO_2 reaction is smaller than that from nocturnal pathways for a given $\Delta^{17}O(NO_2)$ value, as the $\Delta^{17}O$ of OH radical is significantly lower (most case is zero) than that of O_3 in the troposphere [*Chan et al.*, 2021; *Michalski et al.*, 2003; *Savarino and Thiemens*, 1999; *Vicars and Savarino*, 2014; *X Liu et al.*, 2018]. In the context of winter Beijing haze, several observations of $\Delta^{17}O(NO_3^-)$ have been conducted to understand the nitrate production mechanisms [*Fan et al.*, 2022; *He et al.*, 2018; *Song et al.*, 2020; *Y Wang et al.*, 2019]. Based on simple isotope mass-balance models, these isotopic results indicated that the nocturnal pathways (N_2O_5 hydrolysis and NO_3 + HC) dominate nitrate formation during haze days (>70%) [*Fan et al.*, 2022; *He et al.*, 2018; *Y Wang et al.*, 2019], in contrast to results derived from the observation-constrained box model and CTMs which either predicted daytime OH + NO_2 was dominant or N_2O_5 hydrolysis and daytime OH + NO_2 reaction were equally important. In addition, the GEOS-Chem model constrained using observed

$\Delta^{17}O(NO_3^-)$ also predicted the dominance of N_2O_5 hydrolysis in nitrate production in winter Beijing [*Chan et al.*, 2021]. However, the GEOS-Chem model underestimated the observed $\Delta^{17}O(NO_3^-)$ values during extreme haze events [*Chan et al.*, 2021], despite the fact that the same model in general reproduced well the observed $\Delta^{17}O(NO_3^-)$ (sometimes with slight overestimation) in many other locations [*Alexander et al.*, 2020]. The disagreement between the observed and modeled $\Delta^{17}O(NO_3^-)$ in Beijing winter haze events suggests either the contribution of N_2O_5 hydrolysis to nitrate production is still underestimated, or other pathways leading to high $\Delta^{17}O(NO_3^-)$ are omitted or underestimated by the model. In particular, heterogeneous N_2O_5 reaction on Cl^--containing aerosols (heterogeneous $N_2O_5 + Cl^-$ chemistry) would yield nitrate with a higher $\Delta^{17}O(NO_3^-)$ signature compared to nitrate produced from N_2O_5 hydrolysis [*Alexander et al.*, 2020]. But current studies either ignored anthropogenic Cl emission (e.g., *Fu et al.*, 2020) which is important for inland cities [*Thornton et al.*, 2010; *B Zhang et al.*, 2022; *X Wang et al.,* 2020] and/or with uncertain $ClNO_2$ yield from heterogeneous $N_2O_5 + Cl^-$ chemistry [*Chan et al.*, 2021]. The former would underestimate the overall heterogeneous $N_2O_5 + Cl^-$ chemistry, and the latter would underestimate the production of nitrate from heterogeneous $N_2O_5 + Cl^-$ chemistry. Recent field campaigns conducted across China have reported elevated concentrations of N_2O_5 and $ClNO_2$, indicating active $N_2O_5 + Cl^-$ chemistry [*Li et al.*, 2022; *X Liu et al.*, 2017; *H Wang et al.*, 2018b; *X Wang et al.*, 2017; *Xia et al.*, 2020; *Yu et al.*, 2020]. In particular, the observed $ClNO_2$ concentration is several times higher than modeled $ClNO_2$ by Chan et al., 2021 [*Chan et al.*, 2021; *X Wang et al.*, 2017]. Therefore, the contribution of $N_2O_5 + Cl^-$ chemistry to nitrate production and $\Delta^{17}O(NO_3^-)$ in the Beijing winter haze needs to be revisited.

Quantifying the propagation of $\Delta^{17}O$ in NO_x chemistry constrained by observations of key precursors (i.e., OH, RO_2, O_3, NO_x) offers valuable insights into the nitrate formation mechanisms and the associated $\Delta^{17}O(NO_3^-)$ during winter haze events. In this study, field observations of $\Delta^{17}O(NO_3^-)$ near the surface (winter of 2014~2016) and tall tower (winter of 2016, within the framework of the campaign of Air Pollution and Human Health in Chinese Megacities in Beijing (APHH)), as well as radical concentrations and other related parameters are compiled and dissected [*Fan et al.*, 2022; *He et al.*, 2018; *Song et al.*, 2020; *Y Wang et al.*, 2019]. The APHH campaign represents one of the few field observations in urban environments including in-situ

measurements of radicals (OH, HO_2 and RO_2), the OH reactivity, gas and particle pollutants relating to NO_x chemistry, and especially $\Delta^{17}O(NO_3^-)$ measurements in three different layers. With these data, we hope to reconcile the observed $\Delta^{17}O(NO_3^-)$ with improved nitrate chemistry and/or $\Delta^{17}O$ propagations in the NO_x cycle and the subsequent nitrate formations and to better understand the formation mechanisms of nitrate in Beijing winter haze.

2. Data and Methods

2.1 $\Delta^{17}O(NO_3^-)$ and ancillary data in haze events

Observations of $\Delta^{17}O(NO_3^-)$ in Beijing haze, as well as the available meteorological and chemical parameters compiled from the literature, are summarized in Table 1. In total, 128 pairs of $\Delta^{17}O(NO_3^-)$ and $\delta^{15}N(NO_3^-)$ measurements in the winter seasons of Beijing are compiled (see SI). $PM_{2.5}$ samples were either collected near the surface or simultaneously at three heights (8m, 120m, and 260m in the winter of 2016) of a tall tower. During the sampling period of Fan et al., 2022 (November-December, 2016), the OH, HO_2/RO_2 concentrations, OH reactivity (k(OH)), trace gas and aerosol concentration, as well as meteorological conditions were also monitored and available on https://archive.ceda.ac.uk/ (last accessed on November 6, 2022). These field measurements of OH, k(OH), $HO_{2,}$ and RO_2 have been described in detail by Slater et al., 2020 [*Slater et al.*, 2020]. In this study, we mainly focus on haze days with $PM_{2.5}$ concentrations higher than 75 μg m^{-3} (several days with nitrate concentrations higher than 5 μg m^{-3} are also included). This definition has been widely used in many previous studies [*Ma et al.*, 2019].

2.2 Evaluation of $\Delta^{17}O$ of key precursors relating to nitrate formation

The traditional steady-state formalism is used to interpret the measured $\Delta^{17}O(NO_3^-)$, which is expressed by the isotopic mass balance as the following equation:

$$\Delta^{17}O(NO_3^-) = f_i \times (\Delta^{17}O(NO_3^-)_i) \qquad \text{(Equation 1)}$$

where f_i represents the relative contribution of individual reaction to the production of p-NO_3^-, and $(\Delta^{17}O(NO_3^-)_i)$ is the $\Delta^{17}O$ values of nitrate produced through individual reaction. Once the

193    $\Delta^{17}O(NO_3^-)_i$ is determined, the pathway-specific contribution can be resolved using a Bayesian

194   mixing model (named Stable Isotope Mixing Models in R, simmr) [*Phillips et al.*, 2014; *Z Zhang*

195   *et al.*, 2020]. The $\Delta^{17}O(NO_3^-)_i$ can be calculated by accounting for $\Delta^{17}O$ of each intermediate

196   scaled by their transferring factor, e.g., for the potentially important formation pathways in Beijing

197   winter haze, $\Delta^{17}O(NO_3^-)_i$ can be calculated as follows:

198                $\Delta^{17}O(NO_3^-)_{OH+NO2} = 2/3 \times \Delta^{17}O(NO_2)_{day} + 1/3 \times \Delta^{17}O(OH)$ (Equation 2)

199                $\Delta^{17}O(NO_3^-)_{N2O5+H2O} = 4/6 \times \Delta^{17}O(NO_2)_{night} + 1/6 \times \Delta^{17}O(O_3^*)$ (Equation 3)

200                $\Delta^{17}O(NO_3^-)_{N2O5+Cl} = 2/3 \times \Delta^{17}O(NO_2)_{night} + 1/3 \times \Delta^{17}O(O_3^*)$ (Equation 4)

201   Unlike $\Delta^{17}O(O_3)$ which is well constrained by observations [*Ishino et al.*, 2017; *Vicars and*

202   *Savarino*, 2014], the $\Delta^{17}O$ of OH and NO_2 are usually assumed based on theoretical predictions

203   with little to no observational constraints [*Albertin et al.*, 2021]. To better understand the observed

204    $\Delta^{17}O(NO_3^-)$, it is necessary to evaluate the assumed $\Delta^{17}O$ values of OH and NO_2.

205   **2.2.1 $\Delta^{17}O$ of OH radicals in Beijing Haze**

206   Interpretation of observed $\Delta^{17}O(NO_3^-)$ as well as model simulation always set $\Delta^{17}O$ of steady-state

207   OH as zero by assuming OH-H_2O isotope equilibrium is rapidly achieved [*Chan et al.*, 2021],

208   while $\Delta^{17}O$ of OH is expected to be positive when OH loss rate can compete with or outweigh its

209   equilibrium exchange reaction with H_2O [*Savarino et al.*, 2016; *Z Zhang et al.*, 2021b]. Since

210   unprecedentedly high OH oxidation rates have been observed in winter haze events in Beijing [*Lu*

211   *et al.*, 2019; *Slater et al.*, 2020], it is necessary to evaluate whether OH-H_2O isotope equilibrium is

212   achieved or not in Beijing winter haze. Previous study has found that in winter Beijing the OH

213   chemical loss rate can compete with or even outweigh its equilibrium exchange rate with H_2O

214   under conditions of abundant primary pollutants and relatively low water mixing ratios [*Z Zhang*

215   *et al.*, 2021b], implying a possibly positive $\Delta^{17}O$ signature of steady-state OH under such

216   conditions. The steady-state $\Delta^{17}O(OH)$ signature is a function of the initial $\Delta^{17}O(OH)$ upon its

217   formation (denoted $\Delta^{17}O(OH)_{prod}$) and the degree of the isotopic exchange equilibration between

218   OH and H_2O (as β). In this study, using the relevant parameters (i.e., OH loss rate, the source and

sinks of OH) from direct observations or computed using box models constrained by observations that have been reported by Slater et al (2020) [*Slater et al.*, 2020], we calculate the steady-state $\Delta^{17}O(OH)$ in Beijing haze following the same method in Savarino et al., 2016 [*Savarino et al.*, 2016] as follows:

$$\Delta^{17}O(OH) = \beta \times \Delta^{17}O(OH)_{prod} \qquad \text{(Equation 5)}$$

$$\beta = L/(L+E) \qquad \text{(Equation 6)}$$

in which "E" represents the isotopic exchange rate between OH and H_2O, and "L" represents the total loss rate of OH. To calculate the β, the isotopic exchange rate between OH and H_2O recommended by Dubey et al. (1997) is applied [*Dubey et al.*, 1997].

For the estimation of $\Delta^{17}O(OH)_{prod}$ (Eq. 5), a simple isotope mass balance equation is used. Recent wintertime campaigns found that the $HO_2/RO_2 + NO$ recycle reaction (80~90%) and the photolysis of HONO (10~20%) are the most important sources of OH during winter haze days in urban Beijing [*Slater et al.*, 2020]. The pathway of O_3 photolysis is neglected, because its contribution to OH production is negligible (<1%) [*Slater et al.*, 2020]. Usually, the $\Delta^{17}O(OH)$ generated from the recycling process (i.e., $HO_2 + NO$) is predicted to be negligible. The $\Delta^{17}O(OH)_{prod}$ will therefore depend on the $\Delta^{17}O$ of HONO and the fraction of HONO photolysis relative to the total primary source of OH.

$$\Delta^{17}O(OH)_{prod} = f \times \Delta^{17}O(HONO) \qquad \text{(Equation 7)}$$

where f represents the fractional contribution of HONO photolysis to OH formation. An upper limit of the contribution of HONO photolysis (20%) is used in the following discussion [*Slater et al.*, 2020; *Tan et al.*, 2018; *Ma et al.*, 2019].

However, the $\Delta^{17}O$ value of HONO has not been reported and is indeed more difficult to estimate because of the rapid cycling of HONO with NO_x, as well as the different sources involved in HONO formation (i.e., NO_2 conversion on aerosol surfaces and ground, primary emission, nitrate photolysis, etc.) [*Jiang et al.*, 2020; *Xue et al.*, 2020], which are characterized by distinct $\Delta^{17}O$

244 signatures. For instance, the $\Delta^{17}O$ of HONO from the NO_2 heterogeneous reaction can be

245 approximated as $\Delta^{17}O(NO_2)$, assuming a mass-dependent fractionation process during the NO_2

246 heterogeneous reaction. We assume that the $\Delta^{17}O$ of HONO from nitrate photolysis is equal to

247 that of particulate nitrate because the oxygen atoms in HONO can be traced back to the nitrate.

248 The $\Delta^{17}O$ of HONO produced from gas-phase reaction (NO + OH) is approximately half of that of

249 NO. The previous observational-based model study suggested that the NO_2 heterogeneous reaction,

250 the gas-phase reaction of NO with OH, and the photolysis of nitrate are critical daytime HONO

251 sources in urban Beijing [*W Zhang et al.*, 2020]. For simplicity, an upper limit of $\Delta^{17}O(HONO)$

252 corresponding to the daytime $\Delta^{17}O(NO_2)$ is used in this study, which may lead to an overestimate

253 of steady-state $\Delta^{17}O(OH)$.

254 **2.2.2 Evaluation of Daytime and nighttime $\Delta^{17}O(NO_2)$ values**

255 According to the mass-balance model of $\Delta^{17}O(NO_3^-)$ calculations (Eq.2-Eq.4), $\Delta^{17}O(NO_3^-)$ is

256 largely driven by $\Delta^{17}O(NO_2)$. Therefore, a prior understanding of $\Delta^{17}O(NO_2)$ is essential for

257 $\Delta^{17}O(NO_3^-)$ interpretation. Measurements of $\Delta^{17}O(NO_2)$ suggested a radically different NO_2

258 chemistry during the day and at night, resulting in significant contrast of $\Delta^{17}O$ signatures between

259 day and night [*Albertin et al.*, 2021]. However, previous interpretations of observed $\Delta^{17}O(NO_3^-)$ as

260 well as model simulations always use 24-h average NO_2 production rates to calculate the daytime

261 and nighttime $\Delta^{17}O(NO_2)$ and don't consider the potential difference in $\Delta^{17}O(NO_2)$ values in

262 different vertical layers at night [*Alexander et al.*, 2020; *Chan et al.*, 2021]. In urban environments,

263 daytime $\Delta^{17}O(NO_2)$ is predicted to be determined by the O_3 isotopic anomaly and its relative

264 importance in the NO oxidation [*Michalski et al.*, 2014; *Savarino et al.*, 2008]. The daytime

265 $\Delta^{17}O(NO_2)$ can be estimated using Eq. 8:

266
$$\Delta^{17}O(NO_2)_{day} = \Delta^{17}O(O_3^*) \times \frac{k_{NO+O3}[O_3]}{k_{NO+O3}[O_3]+k_{RO2+NO}[RO_2]+k_{HO2+NO}[HO_2]} \qquad \text{(Equation 8)}$$

267 with $\Delta^{17}O(O_3^*)$ being the $\Delta^{17}O$ value of terminal oxygen atoms in ozone (~39.3‰) [*Vicars and*

268 *Savarino*, 2014], and the concentrations of O_3, HO_2, and RO_2 have been measured directly during

269 the APHH campaign [*Slater et al.*, 2020]. This equation assumes NO and NO_2 reach isotope

270 equilibrium given the fast daytime cycling between NO and NO_2. During the daytime,

271    $\Delta^{17}O(NO_2)_{day}$ can represent the well-mixed condition within the boundary layer.

272   At night, the cycling from NO_2 to NO is muted given the absence of sunlight, and nighttime

273   emission of NO at the surface and its conversion to NO_2 will dilute any $\Delta^{17}O(NO_2)$ signatures that

274   survived from the day. Moreover, the strong and stable nighttime stratification during haze events

275   would lead to distinct NO_x chemical regimes (i.e., NO-NO_2 conversion and nitrate formation) at

276   different vertical layers, i.e., the surface layer and the residual layer as illustrated by Fig. 1 [*X*

277   *Chen et al.*, 2020; *Fan et al.*, 2022; *H Wang et al.*, 2018a]. This further complicates the

278   interpretation of nighttime $\Delta^{17}O(NO_2)$ and subsequently the $\Delta^{17}O(NO_3^-)$ signatures. Since NO is

279   mainly emitted from the surface and at winter night it will stay near the surface because radiation

280   inversion leads to vertically stable air near the surface, thereby we assume no fresh NO would

281   enter the residual layer above the surface inversion layer. Therefore, $\Delta^{17}O(NO_2)$ in the residual

282   layer cannot be diluted. In summary, we expect that the nighttime $\Delta^{17}O(NO_2)$ signals also differ

283   between vertical layers. Here we consider the nighttime $\Delta^{17}O(NO_2)$ values are different between

284   the surface (i.e., the bottom of the inversion layer) and the residual layer. We follow *Albertin et al.*,

285   2021 to estimate the surface $\Delta^{17}O(NO_2)$ signatures at night in the polluted urban environment as

286   follows:

287    $$\Delta^{17}O(NO_2)_{surface} = \left\{ \theta \times \Delta^{17}O(NO_2)_{susnset} + (1-\theta) \times \frac{1}{2} \times \Delta^{17}O(O_3^*) \right\} \text{ (Equation 9)}$$

288   where θ is the fraction of daytime leftover NO_x (NO + NO_2) at sunset relative to the total NO_x

289   overnight, and $\Delta^{17}O(NO_2)_{sunset}$ is the oxygen isotope anomaly of NO_2 at sunset that can be

290   estimated according to Eq. 8. The θ is calculated as follows:

291    $$\theta = \frac{C[NO_x]_{left}}{C[NO_x]_{left} + \int_0^t k_{O3+NO}[O_3][NO]\, dt} \text{ (Equation 10)}$$

292   Usually, in urban cities of China (i.e., Beijing) with abundant nighttime NO emissions, θ would be

293   on the order of 1%~5%.

294   For nighttime $\Delta^{17}O(NO_2)$ in the residual layer, a few assumptions are made based on the

295   observations: (1) at night nearly all the NO_x in the residual layers would be converted to NO_2 since

296   NO is quickly oxidized by O_3 (NO lifetime of several minutes) and the surface freshly emitted NO

297   would not disperse into the residual layer [*H Wang et al.*, 2018a]; (2) $\Delta^{17}O(NO_2)$ in the residual

298   layer is composited of $\Delta^{17}O(NO_2)$ at sunset (i.e., daytime leftover NO_2) and newly formed from O_3

299   oxidation of NO leftover from the day. Following *Albertin et al.*, 2021, the nighttime $\Delta^{17}O(NO_2)$

300   in the residual layer can be expressed as:

301   $$\Delta^{17}O(NO_2)_{residual} = \left\{ \rho \times \Delta^{17}O(NO_2)_{sunset} + (1-\rho) \times \frac{\Delta^{17}O(NO)_{sunset} + \Delta^{17}O(O_3^*)}{2} \right\} \text{ (Equation 11)}$$

302   with ρ representing the fraction of NO_2 in total NO_x at sunset, and $\Delta^{17}O(NO)_{sunset}$ would equal to

303   $\Delta^{17}O(NO_2)_{sunset}$ given the photo-driven cycling of NO and NO_2.

304   **3. Results**

305   **3.1 Comparison of observed and modelled $\Delta^{17}O(NO_3^-)$ in winter haze in Beijing**

306   As shown in Figure 2, $\Delta^{17}O(NO_3^-)$ of $PM_{2.5}$ near the surface varies significantly, from 19.6‰ to

307   36.5‰ with mean values of (29.6 ± 3.7) ‰. Compared to surface samples, the $\Delta^{17}O(NO_3^-)$ and

308   p-NO_3^- aloft increase considerably (Fig. S1) [*Fan et al.*, 2022]. $\Delta^{17}O(NO_3^-)$ in surface samples is

309   correlated positively with p-NO_3^- (Fig. 2), as has been reported in previous studies [*Chan et al.*,

310   2021]. However, the CTM modeled $\Delta^{17}O(NO_3^-)$ generally showed a slightly decreasing trend as

311   p-NO_3^- increased [*Chan et al.*, 2021]. Under moderate haze days, the modelled $\Delta^{17}O(NO_3^-)$ is

312   approximately higher by ~2.0‰ than the observed value. In contrast, the modelled $\Delta^{17}O(NO_3^-)$

313   under extreme haze days is lower by 1.6‰ than the observed values, partly because the modelled

314   maximum $\Delta^{17}O(NO_3^-)$ (~31.8‰) is significantly lower than the observed maximum $\Delta^{17}O(NO_3^-)$

315   values [*Chan et al.*, 2021]. The comparison suggests an incomplete understanding of NO_x

316   chemistry and/or the $\Delta^{17}O$ transfer mechanisms under haze days.

317   **3.2 The estimation of $\Delta^{17}O(OH)$**

318   Table S1 presents an example of the mass balance calculation of $\Delta^{17}O(OH)$, and the estimated

319   steady-state $\Delta^{17}O(OH)$ is presented in Figure 3. The calculated β (0.10~0.86) and $\Delta^{17}O(OH)$

320   (1.0‰~6.5‰) show large variations. Both the β and $\Delta^{17}O(OH)$ tend to increase with the increase

321   of $PM_{2.5}$, implying a growing proportion of initial $\Delta^{17}O(OH)$ preserved against exchange with H_2O

322   with the development haze events (Fig. S2). Since the $OH + NO_2$ reaction is the dominant OH loss

323   process [*Slater et al.*, 2020], the calculated steady-state $\Delta^{17}O(OH)$ is also positively and

324   significantly correlated with the NO_2 (Fig. S2). This positive relationship between $\Delta^{17}O(OH)$ and

325   NO_2 indicates that $\Delta^{17}O(OH)$ is potentially important for model underestimation of $\Delta^{17}O(NO_3^-)$.

326   **3.3 The estimation of $\Delta^{17}O(NO_2)$**

327   The diurnal profiles of peroxyl radical mixing ratio, relative humidity (RH), temperature, CO, SO_2,

328   O_3, NO, and NO_2 during the APHH campaign are shown in Fig. S3. Days with available peroxyl

329   radicals cover a wide range of $PM_{2.5}$ concentrations, ensuring our estimated $\Delta^{17}O(NO_2)_{day}$ is

330   representative. The estimated daytime-averaged $\Delta^{17}O(NO_2)_{day}$ is presented in Figure. 4, which

331   ranges from 30.5‰ to 36.6‰ (on average 33.1 ± 2.1‰). Our estimated $\Delta^{17}O(NO_2)_{day}$ is close to

332   the measured daytime $\Delta^{17}O(NO_2)$ in late spring in Grenoble, France (34.5‰) [*Albertin et al.*,

333   2021]. Opposite to $\Delta^{17}O(OH)$, the $\Delta^{17}O(NO_2)_{day}$ is negatively correlated with $PM_{2.5}$, because O_3

334   declines significantly but peroxyl radicals remain constant on haze days [*Slater et al.*, 2020]. It

335   should be noted that our estimated $\Delta^{17}O(NO_2)_{day}$ values are significantly lower than that simulated

336   in the model studies (38.5‰~39.0‰) [*Chan et al.*, 2021; *Alexander et al.*, 2020].

337   Constrained by the observational dataset from the APHH campaign, the estimated nocturnal

338   surface $\Delta^{17}O(NO_2)_{surface}$ value is on average 23.0‰ during haze events. This is consistent with the

339   findings of Albertin et al. (2021), in which a low $\Delta^{17}O(NO_2)$ value averaged of 25.8‰ at night was

340   observed [*Albertin et al.*, 2021]. The small $\Delta^{17}O(NO_2)_{surface}$ value at night is attributed to high

341   nighttime NO emissions associated with a negligible $\Delta^{17}O$ value in the urban polluted

342   environment.

343   In comparison, the calculated $\Delta^{17}O(NO_2)_{residual}$ values in the residual layer at night range from 33.6‰

344   to 39.0‰, with an average of 36.2‰. The high $\Delta^{17}O(NO_2)_{residual}$ can be attributed to the

345   dominance of O_3 in the oxidation of NO, which is associated with a relatively high $\Delta^{17}O$ value

346   reaching isotopic exchange equilibrium with NO_2 at sunset. Nevertheless, our estimated

347      $\Delta^{17}O(NO_2)_{residual}$ is still slightly lower than the model simulated values [*Chan et al.*, 2021;

348   *Alexander et al.*, 2020].

4. Discussion

350   Model simulations constrained by $\Delta^{17}O(NO_3^-)$ suggested that the dominant pathway for nitrate

351   production is N_2O_5 hydrolysis on deliquescent aerosols in urban Beijing during haze events [*Chan*

352   *et al.*, 2021]. However, the model failed to reproduce the observed increasing trend of $\Delta^{17}O(NO_3^-)$

353   with nitrate concentration [*Chan et al.*, 2021]. In particular, the model predicted lower $\Delta^{17}O(NO_3^-)$

354   values compared to the observed values under extreme haze days [*Chan et al.*, 2021]. This

355   underestimation indicates that the understanding of processes or precursors with high $\Delta^{17}O$ values

356   that contribute to nitrate formation is incomplete. To address this discrepancy, potential factors are

357   evaluated separately in the following discussions.

4.1 The effect of $\Delta^{17}O(OH)$

359   Recent field observations have provided evidence of active wintertime photochemistry in urban

360   Beijing, which contributes significantly to the formation of secondary pollutes [*Lu et al.*, 2019;

361   *Tan et al.*, 2018; *Slater et al.*, 2020]. For instance, during the APHH campaign, the measured

362   average OH reactivity and concentration were found to be 47 s^{-1} and $2.7*10^{\wedge 6}$ molecules cm^{-3},

363   respectively [*Slater et al.*, 2020], resulting in an OH loss rate of $12.7*10^{\wedge 7}$ molecules cm^{-3} s^{-1}. In

364   comparison, the average O isotopic exchange rate between OH and H_2O is approximately $9.8*10^{\wedge 7}$

365   molecules cm^{-3} s^{-1}. This comparison suggests that approximately 56% of the $\Delta^{17}O(OH)$ derived

366   from its precursors is preserved against the oxygen isotope equilibrium exchange reaction between

367   OH and H_2O. Additionally, the estimated $\Delta^{17}O(OH)$ tends to increase with the increasing NO_2 and

368   p-NO_3^- levels (Fig. S2), as the OH + NO_2 reaction predominates the OH loss rate [*Slater et al.*,

369   2020]. Therefore, our findings indicate $\Delta^{17}O(OH)$ in Beijing winter haze is likely positive and can

370   in part account for the negative bias of $\Delta^{17}O(NO_3^-)$ predicted by the CTM model, as the model

371   assume a $\Delta^{17}O(OH)$ value of zero.

372   Accounting for the $\Delta^{17}O(OH)$ can increase the modeled $\Delta^{17}O(NO_3^-)$ by ~ 1‰ and note that this is

373   the upper limit. However, the model still falls short of accurately capturing the true extent of

374    $\Delta^{17}O(NO_3^-)$ even with this adjustment. In other words, if the disagreement between the modelled

375 and observed $\Delta^{17}O(NO_3^-)$ (~1.6‰) were solely reconciled by accounting for the $\Delta^{17}O(OH)$, we

376 would expect a substantial rise of $\Delta^{17}O(OH)$ to approximately 9.6‰ on haze days, which

377 significantly exceeds our estimated values that are already at its upper limit. Furthermore,

378 considering that the estimated $\Delta^{17}O(NO_2)_{day}$ is significantly lower than the simulated values by the

379 model, it is highly improbable that the daytime $OH + NO_2$ reaction can account for the model's

380 underestimation of $\Delta^{17}O(NO_3^-)$ in extreme haze days. Consequently, we propose that the observed

381 and modelled $\Delta^{17}O(NO_3^-)$ discrepancy during haze events in Beijing stems from underestimates of

382 some nocturnal NO_x chemistry.

383 **4.2 The effect of nocturnal NO_x chemistry**

384 **4.2.1 The potential effects of nighttime $\Delta^{17}O(NO_2)$ estimation**

385 One finding from the observational-constrained isotopes of nitrate intermediates is that the

386 nighttime $\Delta^{17}O(NO_2)$ in the surface layer is lower than the modelled ones. This can be attributed to

387 the effect of freshly emitted nighttime NO (~0‰), which dilutes the overall $\Delta^{17}O$ of surface NO_x

388 [*Albertin et al.*, 2021]. For example, the nighttime $\Delta^{17}O(NO_2)$ determined in Grenoble, France is

389 significantly lower than the daytime values (25.8‰ *vs* 34.5‰) [*Albertin et al.*, 2021]. It is evident

390 that CTM model simulations significantly overestimate the nighttime surface $\Delta^{17}O(NO_2)$ values to

391 a large extent, as the model assumes nighttime $\Delta^{17}O(NO_2)$ values are similar to those in daytime

392 [*Alexander et al.*, 2020; *Chan et al.*, 2021]. Similar to that at the surface, the

393 observational-constrained $\Delta^{17}O(NO_2)_{residual}$ (36.2‰) at night in the residual layer is also lower than

394 the model simulated values [*Chan et al.*, 2021]. Despite these, the CTM model still underestimates

395 $\Delta^{17}O(NO_3^-)$. This implies the reasons leading to the underestimate may be related to terminal

396 reactions from NO_2 to HNO_3 at night, which include reactions such as $NO_3 + HC$, N_2O_5 hydrolysis,

397 and heterogeneous $N_2O_5 + Cl^-$ chemistry. We evaluate the importance of these reactions in the

398 following sections.

399 **4.2.2 The effects of the $NO_3 + HC$ pathway**

400 The importance of the $NO_3 + HC$ pathway in nitrate production has been a subject of debate

401 among different research approaches. However, both chemical transport models and
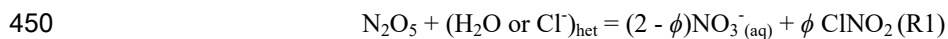
observation-based box models have shown that this pathway does not contribute significantly to nitrate production in winter Beijing haze [*Chan et al.*, 2021; *X Chen et al.*, 2020; *H Wang et al.*, 2018a; *Xie et al.*, 2022; *Zhao et al.*, 2023; *H Wang et al.*, 2021]. For instance, an analysis of the long-term NO_3 radical budget in the winter of 2014-2019 in Beijing demonstrated that N_2O_5 heterogeneous hydrolysis was the dominant process responsible for total NO_3 radical loss, accounting for 77% to 92% [*H Wang et al.*, 2021]. Another study conducted during the APHH campaign revealed that the NO_3 total loss resulting from the reaction with volatile organic compounds (VOCs) contributed less than 5% to the overall removal of NO_x [*Li et al.*, 2022]. Additionally, the oxidation of VOCs by the NO_3 radical favors the production of organic nitrate, as reactions with unsaturated compounds are significantly efficient compared to saturated compounds [*Ng et al.*, 2008]. Due to the low ambient level of organic nitrate, its conversion to inorganic nitrate through hydrolysis only accounts for less than 3% of inorganic nitrate formation globally [*Alexander et al.*, 2020].

However, isotopic studies suggested that NO_3 reacting with VOCs is crucial for nitrate formation, constituting approximately one-third and being particularly important on haze days [*Fan et al.*, 2022; *Y Wang et al.*, 2019; *Zhang et al.*, 2022]. From the view of isotopic signature, the contribution of the NO_3 + HC channel is difficult to distinguish from the N_2O_5 + Cl⁻ channel as these two pathways exhibit similar $\Delta^{17}O$ endmembers [*Fan et al.*, 2022; *He et al.*, 2018; *Alexander et al.*, 2020]. Moreover, relying solely on the $\Delta^{17}O$ tracer to estimate multiple pathways' contributions may introduce significant uncertainties [*Phillips et al.*, 2014]. To address this, the evaluation of the $\Delta^{17}O–\delta^{15}N$ (or $\delta^{18}O–\delta^{15}N$) array of p-$NO_3^-$ can provide valuable insights [*Walters and Michalski*, 2016; *Z Zhang et al.*, 2021a]. Theoretically, the N_2O_5 + H_2O and N_2O_5 + Cl⁻ pathways will result in enrichments in $\delta^{15}N$ of nitrate while the NO_3 + HC pathway will cause depletions in $\delta^{15}N$ of nitrate compared to the precursors [*Walters and Michalski*, 2015]. In terms of $\Delta^{17}O$, the NO_3 + HC and N_2O_5 + Cl⁻ pathways will produce more enriched oxygen anomaly, approximately 6.5‰ higher than the N_2O_5 + H_2O pathway (~1/6 of $\Delta^{17}O(O_3^*)$). Consequently, the more significant the NO_3 + HC pathways, the more negative the slopes of $\Delta^{17}O$ against $\delta^{15}N$ in nitrate. Based on these findings, Zhang et al., 2021 reported that the NO_3 + HC pathway accounted for an average of only 8% of wintertime (2017-2018) nitrate production in Beijing [*Z Zhang et al.*,

431 2021b], which aligns with the results obtained from atmospheric transport models and

432 observation-based box models. Re-analysis of paired $\Delta^{17}O$ and $\delta^{15}N$ values from existing literature

433 demonstrates positive linear relationships (Fig. S4), suggesting that the NO_3 + HC pathway may

434 play a minor role in wintertime nitrate formation in the NCP region.

435 **4.2.3 The potential contribution of heterogeneous N_2O_5 + Cl^- chemistry**

436 Recent field observations in the NCP region have revealed elevated levels of $ClNO_2$, suggesting

437 the prominent role of the N_2O_5 + Cl^- pathways in nitrate formation as $ClNO_2$ is a byproduct of

438 heterogeneous N_2O_5 + Cl^- chemistry (R1-R2) [*Tham et al.*, 2018; *Xia et al.*, 2021; *Yan et al.*, 2019;

439 *Yu et al.*, 2020]. In addition, the presence of $ClNO_2$ can significantly affect the regional

440 atmospheric oxidation capacity. For instance, Yang et al., 2022 estimated that the $ClNO_2$ chemistry

441 can increase the surface O_3 by up to 4.5ppbv across China [*Yang et al.*, 2022]. However, the field

442 campaign-derived yield of $ClNO_2$ (ϕ in R1) from heterogeneous N_2O_5 + Cl^- chemistry shows large

443 variations, ranging from 0.01 to 0.73 across China (Table 2). In addition to the traditional

444 laboratory experiment or field observational approach, we propose that nitrate $\Delta^{17}O$ composition

445 at night may be used to constrain the yield of $ClNO_2$ (ϕ) because the nighttime $\Delta^{17}O(NO_3^-)$ values

446 depend on the branching ratio of $ClNO_2$ production that represents the relative importance of N_2O_5

447 + H_2O and N_2O_5 + Cl^- pathways. In particular, the nighttime $\Delta^{17}O(NO_3^-)$ endmembers will be

448 approximately 30.7‰ when $\phi = 0$, while it will be approximately 37.2‰ when $\phi = 1$, considering

449 that the $\Delta^{17}O(NO_2)$ in the residual layer is calculated to be 36.2‰ during haze days.

450 $$N_2O_5 + (H_2O \text{ or } Cl^-)_{het} = (2 - \phi)NO_3^-{}_{(aq)} + \phi\ ClNO_2\ (R1)$$

451 $$ClNO_2 + h\nu \rightarrow Cl + NO_2\ (R2)$$

452 Since nocturnal nitrate formation in the surface layer is negligible on haze days relative to the

453 residual layer [*X Chen et al.*, 2020; *H Wang et al.*, 2018b], we can estimate the $\Delta^{17}O(NO_3^-)$

454 endmember aloft by comparing the mass-weighted difference of $\Delta^{17}O(NO_3^-)$ between daily $PM_{2.5}$

455 samples at the surface and in the residual layer (Text S2). Consequently, the derived nighttime

456 $\Delta^{17}O(NO_3^-)$ endmembers were on average 34.6‰ (Text S2). Therefore, the average contributions

457 of N_2O_5 + Cl^- and N_2O_5 + H_2O pathways to nighttime nitrate formation at the residual layer are

458   estimated to be about 60% and 40%, respectively, corresponding to an average yield ratio of

459   ClNO$_2$ at approximately 0.75 (Text S2). Our isotopic approach-derived yield ratio of ClNO$_2$ aligns

460   with the higher end of previous studies (Table 2). The relatively high ClNO$_2$ yield can be

461   attributed to the significant availability of chloride in PM$_{2.5}$ from anthropogenic sources (average

462   of 0.04μg/m^3, corresponding to 5.6M in the aerosol aqueous phase from the ISORROPIA-II model)

463   [*Fan et al.*, 2022; *Thornton et al.*, 2010; *X Wang et al.*, 2023; *B Zhang et al.*, 2022], as laboratory

464   experiments or field observations suggest that the yield of ClNO$_2$ is primarily determined by the

465   concentration of available Cl$^-$[*Bertram and Thornton*, 2009; *Yu et al.*, 2020].

466   The high product yield of ClNO$_2$ estimated in this study implies an elevated mixing ratio of

467   ClNO$_2$ during winter haze days. In fact, previous studies frequently observed high mixing ratios of

468   ClNO$_2$ (i.e., above 0.5 ppbv) in the NCP region in winter [*Xia et al.*, 2021 and reference therein].

469   Noted that the photolysis of ClNO$_2$ and its subsequent reactions (RS1-RS5, Text S3) in the next

470   morning have a significant impact on the budget of ozone, the fate of pollutants, and the oxygen

471   isotope transfer among O-bearing molecules [*Savarino et al.*, 2016; *Thornton et al.*, 2010]. It is

472   expected that the oxidation of NO by ClO will increase the daytime $\Delta^{17}O(NO_2)$ and $\Delta^{17}O(NO_3^-)$

473   because the $\Delta^{17}O$ of ClO is equal to $\Delta^{17}O(O_3)_{terminal}$. Although the oxidation rate of NO + ClO is

474   much higher than that of NO + O$_3$ by approximately three orders of magnitude, its effect on the

475   daily $\Delta^{17}O(NO_2)$ is estimated to be small due to the extremely low ClO concentrations in winter in

476   Beijing (on the order of 10^6 cm^{-3}) [*Li et al.*, 2021]. Similarly, the uptake of ClNO$_3$ is unlikely to

477   significantly impact the daytime $\Delta^{17}O(NO_3^-)$ for two reasons:1) the reaction rate of ClO with NO$_2$

478   is slower than the OH + NO$_2$ reaction under the typical wintertime conditions in Beijing (3.0*10^{-12}

479   cm^3 molecule^{-1} s^{-1} *versus* 1.3*10^{-11} cm^3 molecule^{-1} s^{-1}) [*Seinfeld and Pandis*, 2016]; 2) the

480   photolysis rate of ClONO$_2$ during daytime is much higher than its hydrolysis rate by three orders

481   of magnitude [*Le Breton et al.*, 2018; *Peng et al.*, 2022; *Stimpfle et al.*, 1999]. In summary, our

482   findings suggest that the heterogeneous N$_2$O$_5$ + Cl$^-$ chemistry may play a crucial role in nitrate

483   formation during winter haze in Beijing.

484   **4.3 Implications for nitrate formation pathways in winter haze days**

485   We employ a Bayesian mixing model of simmr to resolve the relative contribution of major nitrate

486   formation pathways (Text S4). The daytime $\Delta^{17}O(NO_3^-)$ endmembers are estimated to be (23.7 ±

487   1.9) ‰ during haze days by accounting for the transfer of the daytime $\Delta^{17}O$ of NO_2 and OH (Eq.

488   2). The average nocturnal $\Delta^{17}O(NO_3^-)$ endmember of 34.6‰ is used by considering an average

489    $ClNO_2$ yield of 0.75 (ϕ in R1) during heterogeneous $N_2O_5 + Cl^-$ chemistry. The high $ClNO_2$ yield

490   used in this study is consistent with the observed high concentrations of $ClNO_2$ (up to several

491   ppbv) in field campaigns over China which are difficult to reconcile with lower $ClNO_2$ yield [*Xia*

492   *et al., 2021* and reference therein]. With these endmembers, we estimate the average contributions

493   of daytime pathways vs. nocturnal pathways to nitrate production in haze events.

494   For $PM_{2.5}$ samples collected at the surface, we estimate that the gas phase OH oxidation pathway

495   (i..e, the daytime pathway) contributes significantly to the particulate nitrate accumulation, with an

496   average of 55% on haze days during the winter seasons of 2014-2016 (Fig. 5). The percentage of

497   nocturnal nitrate pathways in nitrate formation in surface $PM_{2.5}$ samples, on average, is 45% and

498   where 27% is from the $N_2O_5 + Cl^-$ pathway and 18% is from the $N_2O_5 + H_2O$ pathway. It should be

499   noted that the contribution of nocturnal nitrate pathways to nitrate production in the planteary

500   boundary layer may be underestimated when isotope date from only surface $PM_{2.5}$ samples is used,

501   as the surface samples do not fully represent nocturnal nitrate chemistry, i.e., the chemically inert

502   air masses near the surface due to O_3 titration would suppress nocturnal nitrate formation while

503   above the surface layer in the residual layer nocturnal nitrate formation may be still active [*X Chen*

504   *et al.*, 2020; *H Wang et al.*, 2018a].

505   When consider $\Delta^{17}O(NO_3^-)$ data from samples collected at higher altitudes representing the

506   residual layer at night, the importance of N_2O_5 heterogeneous chemistry increases. According to

507   our estimates, on average, approximately 72% of nitrate formation in daily $PM_{2.5}$ samples

508   collected at 260m (i.e., in the residual layer at night) can be attributed to N_2O_5 heterogeneous

509   chemistry (43% for $N_2O_5 + Cl^-$ pathway and 29% for $N_2O_5 + H_2O$ pathway), while the gas phase

510   OH oxidation pathway only accounts for approximately 28% of the particulate nitrate formation.

511   However, it's important to consider samples from the residual layer with the surface layer together

512   as aerosols from these two layers get mixed after sunrise and contribute to nitrate in the entire

513   planteary boundary layer. Considering the scaling ratio of the residual layer to the boundary layer

is approximately 0.5-0.75 in pollution periods in Beijing [*X Chen et al.*, 2020], we find nocturnal

pathways contribute 56%-65% of total nitrate budget in the boundary layer and the rest is from

OH pathway.

Therefore, in order to accurately determine nitrate formation mechanisms, it is essential to

consider not only the pathway-specific $\Delta^{17}O$ endmembers but also the proper aerosol samples that

are representatives of different vertical layers where the chemistry is very different at night. It

should be cautioned to avoid sampling biases that can arise from collecting samples exclusively at

the surface or higher altitudes. Such biases can disproportionately influence the assessment of the

contributions of nocturnal pathways to nitrate budget due to nighttime stratification. For instance,

field observations and model simulations have consistently highlighted the predominant role of

N_2O_5 heterogeneous chemistry in the residual layer compared to the surface layer [*Benton et al.*,

2010; *S Brown et al.*, 2007; *S Brown et al.*, 2013; *Prabhakar et al.*, 2017]. Therefore, incorporating

mass-weighted nitrate $\Delta^{17}O$ signatures from different layers would provide a more representative

understanding of the processes involved.

5. Conclusion

Nitrate has been playing an increasingly significant role in $PM_{2.5}$ pollution, despite the substantial

reduction in NO_x emissions in China. The subdued response of the nitrate to NO_x emission

reductions in recent years can be attributed to the increased levels of photochemical oxidants and

the extended atmospheric lifetime of nitrate. The former influence the conversion mechanisms

from NO_x to nitrate. However, there is still uncertainty regarding the relative importance of the

OH oxidation pathway and the N_2O_5 heterogeneous chemistry in nitrate formation in winter haze

events.

The use of $\Delta^{17}O(NO_3^-)$ has been proposed as a valuable tool for assessing nitrate formation

mechanisms. Nevertheless, the GEOS-Chem model constrained using $\Delta^{17}O(NO_3^-)$ consistently

underestimates the observed $\Delta^{17}O(NO_3^-)$ during severe haze periods in urban Beijing. This

discrepancy suggests that our current understanding of processes or precursors with high $\Delta^{17}O$

values that contribute to nitrate formation is incomplete. To address this, the potential factors (i.e.,

541    $\Delta^{17}O(NO_2)$, $\Delta^{17}O(OH)$, and nitrate formation pathways) are evaluated separately which are

542   constrained using parameters related to NO_x chemistry such as NO_x, O_3, OH, HO_2, RO_2, and OH

543   reactivity. Our findings indicate that the model underestimation of $\Delta^{17}O(NO_3^-)$ can be reconciled

544   by considering the impact of heterogeneous $N_2O_5 + Cl^-$ chemistry, which is associated with higher

545    $\Delta^{17}O$ values. The average contribution of heterogeneous $N_2O_5 + Cl^-$ pathways to nocturnal nitrate

546   formation is estimated to be 60%, corresponding to an average $ClNO_2$ yield of 0.75. The estimated

547   high product yield of $ClNO_2$ is somewhat consistent with the observed high mixing ratios of

548    $ClNO_2$ during winter haze days (i.e., above 0.5 ppbv) in the NCP region in winter. This high yield

549   and subsequent high concentration of $ClNO_2$ imply the potential importance of Cl chemistry not

550   only in nitrate production in winter Beijing haze but also in the oxidation environment.

551   In addition, the vertical difference in $\Delta^{17}O(NO_3^-)$ of samples collected at the surface and the

552   residual layer may indicate the different chemistry in these two layers, where the surface layer is

553   chemically inert compared to the residual layer due to surface O_3 titration at night in winter haze.

554   As such, using $\Delta^{17}O(NO_3^-)$ to constrain nitrate formation pathways should consider proper

555   sampling strategies to make the samples more representative of the entire boundary layer

556   especially doing diurnal or higher resolution sampling and studies.

557   Meanwhile, we note it is important to acknowledge that there are several uncertainties when

558   inferring nitrate formation pathways using the oxygen mass balance equation of atmospheric

559   nitrate, particularly related to assumptions about the $\Delta^{17}O$ values of key precursors (OH, NO_2) and

560   the $\Delta^{17}O$ transfer function. For instance, our analysis revealed that in typical urban polluted

561   environments, the steady-state OH should exhibit a positive $\Delta^{17}O$, as the chemical rate of OH loss

562   can compete with OH exchange with H_2O. In addition, the observed $\Delta^{17}O(NO_2)$ constrained using

563   observational data (O_3 and RO_2) is significantly lower than the values simulated by the model.

564   Given NO_2 is a central species in the atmospheric reactive nitrogen cycle and atmospheric

565   oxidation capacity, quantifying $\Delta^{17}O(NO_2)$ should be given priority to improve understanding of

566   NO_x chemistry in urban polluted environments.

567   **Open research**

568   The nitrate isotope datasets (PM$_{2.5}$ samples collected in Beijing in winter seasons) used in this

569   analysis are described in Chan et al. (2021) and Fan et al., (2021), which are publicly available at

570   http://hdl.handle.net/1773/46927 and https://osf.io/w4png/. The meteorological and atmospheric

571   chemistry parameters used in this analysis are described by Slater et al., (2020)　and are publicly

572   available at https://archive.ceda.ac.uk/.

573   **Conflicts of interest**

574   The authors declare that they have no conflicts of interest

581
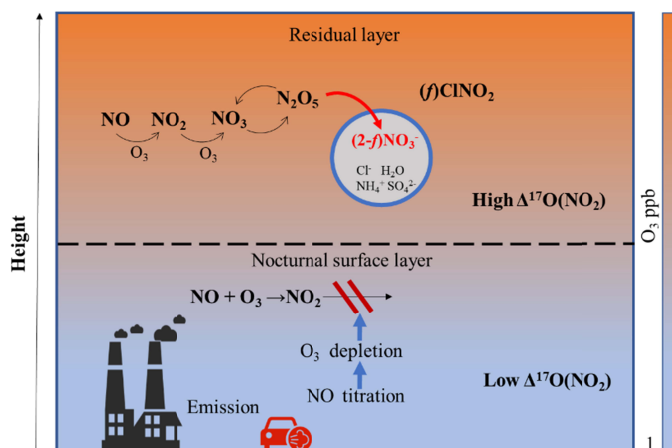
Figure 1. Schematic description of nocturnal NO_x chemistry at different layers during haze episodes. The surface air masses are chemically inert as ozone will be fully titrated by freshly emitted NO. In comparison, the residual layer air masses are chemically reactive, in which the fast N_2O_5 heterogeneous chemistry promotes nitrate accumulation. The O_3 concentrations at different heights were referred from HC Wang et al., 2018.

587
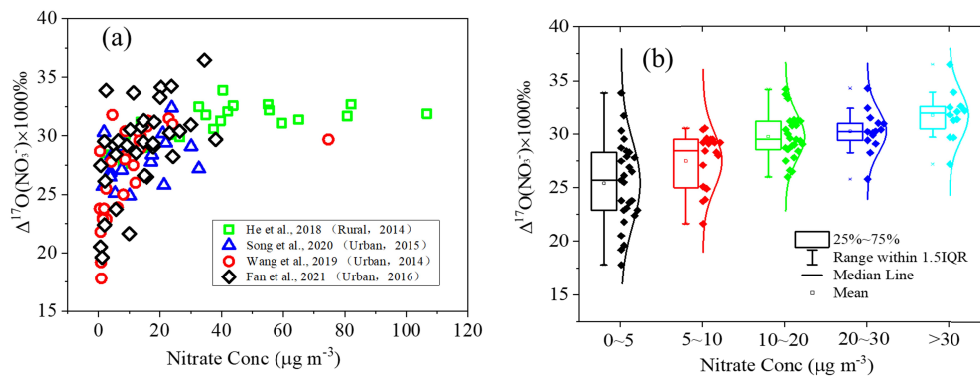
Figure 2. The relationship between $\Delta^{17}O(NO_3^-)$ and NO_3^- concentrations in surface $PM_{2.5}$ samples in urban Beijing. Panel (a) is the scatter plot $\Delta^{17}O(NO_3^-)$ versus NO_3^- concentrations in the previous reports. The boxplot in panel (b) is the statistics of $\Delta^{17}O(NO_3^-)$ in each nitrate regime.

591
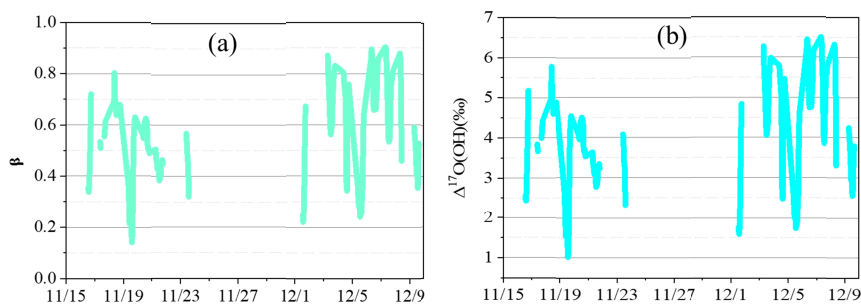
Figure 3. The time series of β (panel a) and $\Delta^{17}O(OH)$ (panel b) during the APHH campaign (2016 winter in urban Beijing). β represents the degree of OH exchange with H_2O relative to the OH isotope exchange rate and its total loss rate. The OH total loss rate is measured online using the laser flash photolysis pump-probe technique.

596

597

598
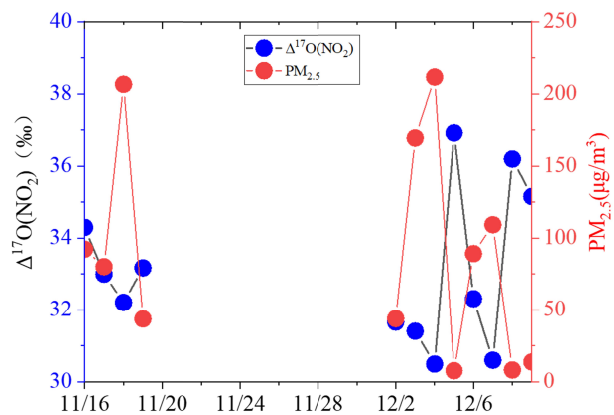
Figure 4. The time series of calculated $\Delta^{17}O(NO_2)$ during the APHH campaign (2016 winter in urban Beijing). The peroxyl radicals and O_3 concentrations were directly measured during the APHH campaign period.

602
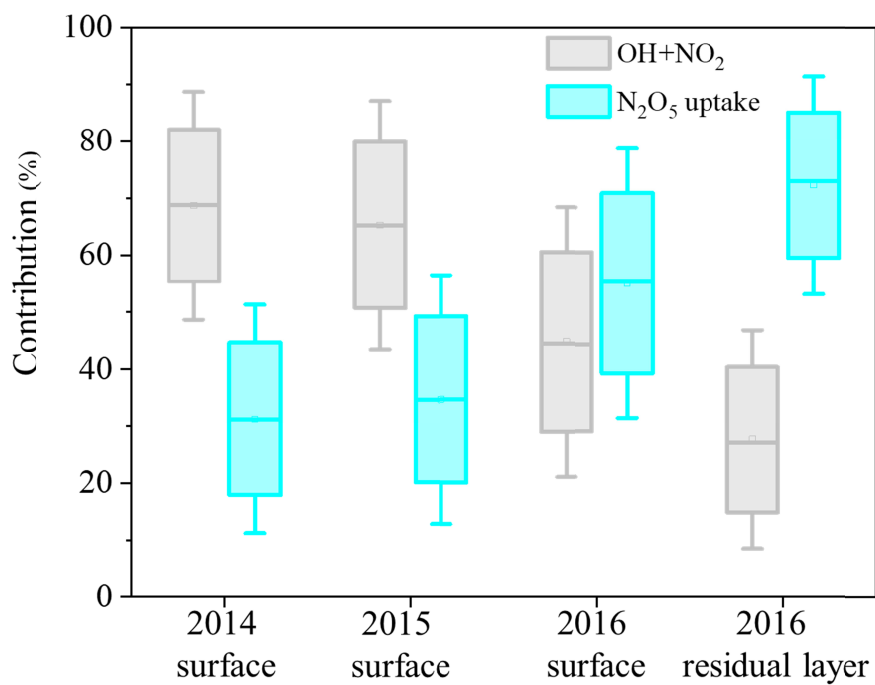
Figure 5. Fractional contributions (mean ± SD values) of daytime OH + NO$_2$ and nocturnal N$_2$O$_5$ uptake pathways to wintertime nitrate production at the surface (2014, 2015, and 2016) or residual layer (2016).

605 Table 1. Compiled data including field observation and model simulation regarding the nitrate
606 formation mechanisms. All the field campaigns were conducted in Beijing from 2014-2016.
607
608

Data	Site	Period	References
$\Delta^{17}O(NO_3^-)$;	IAP	November-December 2016	Fan et al., 2021
p-NO_3^-;	CRAES	November-December 2014	Wang et al., 2019
(Field observation)	CRAES	January 2015	Song et al., 2020
	UCAS-Huairou	October – November 2014	He et al., 2017
$\Delta^{17}O(NO_3^-)$	Nested-grid		
(Model simulation)	simulations for	Winter 2014–2015	Chan et al., 2022
	East Asia		
Radical concentration;			
OH reactivity rate;	IAP	November-December 2016	Slater et al., 2020
O_3、 NO、 NO_2、 $PM_{2.5}$;			
Meteorological parameters			

609
610

611 Table 2. The yield of $ClNO_2$ in previous field campaign that have taken place in China and several
612 model results.

Date	Location	φ $ClNO_2$	Notes	Reference
Sep 2014	Jinan, NCP (urban)	0.014/0.082	Observation-derived	[*Xinfeng Wang et al.*, 2017b]
Dec 2017	Wangdu (rural)	0.06	Observation-derived	[*Xia et al.*, 2021]
Jun 2017	Beijing (urban)	0.10-0.35	Observation-derived	[*Zhou et al.*, 2018]
Jan 2017	Heshan(semi-rural), PRD	0.18-0.32	Observation-derived	[*Hui Yun et al.*, 2018b]
Apr-May 2017	Beijing (urban)	0.05-0.68	Observation-derived	[*Xia et al.*, 2019]
Jan-Feb 2018	Beijing (urban)	0.25± 0.24	Observation-derived	[*Xia et al.*, 2021]
Jul 2014	Mt.Tai, NCP	0.28±0.24	Observation-derived	[*Z Wang et al.*, 2017]
Jun-Jul 2014	Wangdu(rural), NCP	0.34±0.28	Observation-derived	[*Tham et al.*, 2018]
Dec 2013	Mt. Tai Mo Shan in Hongkong	0.43±0.16	Observation-derived	[*H. Yun et al.*, 2018a]
Apr 2018	Nanjing, (suburban) Eastern China	0.56±0.20	Observation-derived	[*Xia et al.*, 2020]
2014-2018	Four sites [a]	0.57 ± 0.33	Fitted field data	[*Yu et al.*, 2020]
2018	Beijing (urban)	0.6-0.8 (annua mean)	Parameterization base on Yu et al.,2020	[*Yang et al.*, 2022]
Oct 2019	Yangmeikeng(rural), PRD	0.71 ± 0.26	Observation-derived	[*Niu et al.*, 2022]
May-Jun 216	Beijing (urban)	0.73 ± 0.25	Observation-derived	[*H Wang et al.*, 2018b]
Sep 2006	Yufa (rural), NCP	0.74 (mean)	Parameterization	[*H Wang et al.*, 2017a]

613 [a]:Four sites include the semirural site (Heshan) in southern China, Mt. Tai in northern China, the rural site at
614 Wangdu, and Mt. Tai Mo Shan in South China.
615
616
617
618
619
620
621
622
623
624
625
626
627
628

629

Reference

Albertin, S., J. Savarino, S. Bekki, A. Barbero, and N. Caillon (2021), Measurement report: Nitrogen isotopes (δ^{15}N) and first quantification of oxygen isotope anomalies (Δ^{17}O, δ^{18}O) in atmospheric nitrogen dioxide, *Atmos. Chem. Phys.*, *21*(13), 10477-10497.

Alexander, B., M. Hastings, D. Allman, J. Dachs, J. Thornton, and S. Kunasek (2009), Quantifying atmospheric nitrate formation pathways based on a global model of the oxygen isotopic composition (Δ^{17}O) of atmospheric nitrate, Atmos. Chem. Phys., 9(14), 5043-5056.

Alexander, B., T. Sherwen, C. D. Holmes, J. A. Fisher, Q. Chen, M. J. Evans, and P. Kasibhatla (2020), Global inorganic nitrate production mechanisms: comparison of a global model with nitrate isotope observations, *Atmos. Chem. Phys.*, *20*(6), 3859-3877.

Benton, A. K., J. M. Langridge, S. M. Ball, W. J. Bloss, M. Dall'Osto, E. Nemitz, R. M. Harrison, and R. L. Jones (2010), Night-time chemistry above London: measurements of NO_3 and N_2O_5 from the BT Tower, *Atmos. Chem. Phys.*, *10*(20), 9781-9795, doi:10.5194/acp-10-9781-2010.

Bertram, T. H., and J. A. Thornton (2009), Toward a general parameterization of N_2O_5 reactivity on aqueous particles: the competing effects of particle liquid water, nitrate and chloride, *Atmos. Chem. Phys.*, *9*(21), 8351-8363, doi:10.5194/acp-9-8351-2009.

Brown, S., W. Dubé, H. Osthoff, D. Wolfe, W. Angevine, and A. Ravishankara (2007), High resolution vertical distributions of NO_3 and N_2O_5 through the nocturnal boundary layer, *Atmos. Chem. Phys.*, *7*(1), 139-149.

Brown, S. S., et al. (2013), Nitrogen, Aerosol Composition, and Halogens on a Tall Tower (NACHTT): Overview of a wintertime air chemistry field study in the front range urban corridor of Colorado, *J. Geophys. Res.-Atmos.*, *118*(14), 8067-8085, doi:10.1002/jgrd.50537.

Chan, Y. C., M. J. Evans, P. He, C. D. Holmes, L. Jaeglé, P. Kasibhatla, X. Y. Liu, T. Sherwen, J. A. Thornton, and X. Wang (2021), Heterogeneous nitrate production mechanisms in intense haze events in the North China Plain, *J. Geophys. Res.-Atmos.*, *126*(9), e2021JD034688.

Chen, D., Z. Liu, J. Fast, and J, Ban (2016), Simulations of sulfate–nitrate–ammonium (SNA) aerosols during the extreme haze events over northern China in October 2014, *Atmos. Chem. Phys. 16*(16), 10707-10724.

Chen, X., H. Wang, K. Lu, C. Li, T. Zhai, Z. Tan, X. Ma, X. Yang, Y. Liu, and S. Chen (2020), Field Determination of Nitrate Formation Pathway in Winter Beijing, *Environ. Sci. Tech.*, *54.15*, 9243-9253.

Cheng, J., J. Su, T. Cui, X. Li, X. Dong, F. Sun, Y. Yang, D. Tong, Y. Zheng, and Y. Li (2019), Dominant role of emission reduction in $PM_{2.5}$ air quality improvement in Beijing during 2013–2017: a model-based decomposition analysis, *Atmos. Chem. Phys.*, *19*(9), 6125-6146.

Dubey, M. K., R. Mohrschladt, N. M. Donahue, and. J. G. Anderson (1997), Isotope Specific Kinetics of Hydroxyl Radical (OH) with Water (H_2O): Testing Models of Reactivity and Atmospheric Fractionation, Journal of Physical Chemistry A *101*(8), 1494-1500.

Fan, M. Y., Y. L. Zhang, Y. C. Lin, Y. Hong, Z. Y. Zhao, F. Xie, W. Du, F. Cao, Y. Sun, and P. Fu (2022), Important Role of NO_3 Radical to Nitrate Formation Aloft in Urban Beijing: Insights from Triple Oxygen Isotopes Measured at the Tower, *Environ Sci Technol*, *56*(11), 6870-6879, doi:10.1021/acs.est.1c02843.

Fu, X., T. Wang, J. Gao, P. Wang, Y. Liu, S. Wang, B. Zhao, and L. Xue (2020), Persistent Heavy Winter Nitrate Pollution Driven by Increased Photochemical Oxidants in Northern China, *Environ. Sci. Tech.*, *54*(7), 3881-3889.

673 Geng, L., L. T. Murray, L. J. Mickley, P. Lin, Q. Fu, A. J. Schauer, and B. Alexander (2017), Isotopic

674 evidence of multiple controls on atmospheric oxidants over climate transitions, *Nature*, *546*(7656),

675 133-136, doi:10.1038/nature22340.

676 Guo, H., J. Liu, K. D. Froyd, J. M. Roberts, P. R. Veres, P. L. Hayes, J. L. Jimenez, A. Nenes, and R. J.

677 Weber (2017), Fine particle pH and gas–particle phase partitioning of inorganic species in Pasadena,

678 California, during the 2010 CalNex campaign, *Atmos. Chem. Phys.*, *17*(9), 5703-5719,

679 doi:10.5194/acp-17-5703-2017.

680 Hastings, M. G. (2004), Seasonal variations in N and O isotopes of nitrate in snow at Summit,

681 Greenland: Implications for the study of nitrate in snow and ice cores, *J. Geophys. Res.-Atmos.*,

682 *109*(D20), doi:10.1029/2004jd004991.

683 He, P., Z. Xie, X. Chi, X. Yu, S. Fan, H. Kang, C. Liu, and H. Zhan (2018), Atmospheric $\Delta^{17}O(NO_3^-)$

684 reveals nocturnal chemistry dominates nitrate production in Beijing haze, *Atmos. Chem. Phys.*, *18*(19),

685 14465-14476, doi:10.5194/acp-18-14465-2018.

686 Ishino, S., S. Hattori, J. Savarino, B. Jourdain, S. Preunkert, M. Legrand, N. Caillon, A. Barbero, K.

687 Kuribayashi, and N. Yoshida (2017), Seasonal variations of triple oxygen isotopic compositions of

688 atmospheric sulfate, nitrate, and ozone at Dumont d'Urville, coastal Antarctica, *Atmos. Chem. Phys.*,

689 *17*(5), 3713-3727, doi:10.5194/acp-17-3713-2017.

690 Jiang, Y., et al. (2020), Sources of nitrous acid (HONO) in the upper boundary layer and lower free

691 troposphere of the North China Plain: insights from the Mount Tai Observatory, *Atmos. Chem. Phys.*,

692 *20*(20), 12115-12131, doi:10.5194/acp-20-12115-2020.

693 Le Breton, M., et al. (2018), Chlorine oxidation of VOCs at a semi-rural site in Beijing: significant

694 chlorine liberation from $ClNO_2$ and subsequent gas- and particle-phase Cl–VOC production, *Atmos.*

695 *Chem. Phys.*, *18*(17), 13013-13030, doi:10.5194/acp-18-13013-2018.

696 Leung, D. M., et al. (2020), Wintertime Particulate Matter Decrease Buffered by Unfavorable Chemical

697 Processes Despite Emissions Reductions in China, *Geophys. Res. Lett.*, *47*(14),

698 doi:10.1029/2020gl087721.

699 Li, Q., et al. (2021), Halogens Enhance Haze Pollution in China, *Environ Sci Technol*, *55*(20),

700 13625-13637, doi:10.1021/acs.est.1c01949.

701 Li, Z., D. Wang, P. Xie, R. Hu, H. Chen, and C. Lin (2022), Nighttime N_2O_5 chemistry in an urban site

702 of Beijing in winter based on the measurements by cavity ring-down spectroscopy, *Air Quality,*

703 *Atmosphere & Health*, *15*(5), 867-876, doi:10.1007/s11869-021-01125-4.

704 Liu, M., F. Shang, X. Lu, X. Huang, Y. Song, B. Liu, Q. Zhang, X. Liu, J. Cao, and T. Xu (2022),

705 Unexpected response of nitrogen deposition to nitrogen oxide controls and implications for land carbon

706 sink, *Nat. Commun.*, *13*(1), 1-10.

707 Liu, M., Y. Song, T. Zhou, Z. Xu, C. Yan, M. Zheng, Z. Wu, M. Hu, Y. Wu, and T. Zhu (2017), Fine

708 particle pH during severe haze episodes in northern China, *Geophys. Res. Lett.*, *44*(10), 5213-5221,

709 doi:10.1002/2017gl073210.

710 Liu, X., et al. (2017), High Levels of Daytime Molecular Chlorine and Nitryl Chloride at a Rural Site

711 on the North China Plain, *Environ Sci Technol*, *51*(17), 9588-9595, doi:10.1021/acs.est.7b03039.

712 Liu, X.-Y., K. Koba, L. A. Koyama, S. E. Hobbie, M. S. Weiss, Y. Inagaki, G. R. Shaver, A. E. Giblin,

713 S. Hobara, and K. Nadelhoffer (2018), Nitrate is an important nitrogen source for Arctic tundra plants,

714 *Proceedings of the National Academy of Sciences*, *115*(13), 3398-3403.

715 Lu, K., H. Fuchs, A. Hofzumahaus, Z. Tan, H. Wang, L. Zhang, S. H. Schmitt, F. Rohrer, B. Bohn, and

716 S. Broch (2019), Fast Photochemistry in Wintertime Haze: Consequences for Pollution Mitigation

717   Strategies, *Environ. Sci. Tech.*, *53*(18), 10676-10684.

718   Ma, X., Z. Tan, K. Lu, X. Yang, Y. Liu, S. Li, X. Li, S. Chen, A. Novelli, and C. Cho (2019), Winter

719   photochemistry in Beijing: Observation and model simulation of OH and HO_2 radicals at an urban site,

720   *Sci. Total. Environ.*, *685*, 85-95.

721   Michalski, G., S. Bhattacharya, and G. Girsch (2014), NOx cycle and the tropospheric ozone isotope

722   anomaly: an experimental investigation, *Atmos. Chem. Phys.*, *14*(10), 4935-4953.

723   Michalski, G., Z. Scott, M. Kabiling, and M. H. Thiemens (2003), First measurements and modeling of

724    $\Delta^{17}O$ in atmospheric nitrate, *Geophys. Res. Lett.*, *30*(16), 1870.

725   Morin, S., J. Savarino, M. M. Frey, N. Yan, S. Bekki, J. W. Bottenheim, and J. M. Martins (2008),

726   Tracing the origin and fate of NOx in the Arctic atmosphere using stable isotopes in nitrate, *Science*,

727   *322*(5902), 730-732, doi:10.1126/science.1161910.

728   Ng, N., A. Kwan, J. Surratt, A. Chan, P. Chhabra, A. Sorooshian, H. O. Pye, J. Crounse, P. Wennberg,

729   and R. Flagan (2008), Secondary organic aerosol (SOA) formation from reaction of isoprene with

730   nitrate radicals (NO_3), *Atmos. Chem. Phys.*, *8*(14), 4117-4140.

731   Niu, Y. B., B. Zhu, L. Y. He, Z. Wang, X. Y. Lin, M. X. Tang, and X. F. Huang (2022), Fast Nocturnal

732   Heterogeneous Chemistry in a Coastal Background Atmosphere and Its Implications for Daytime

733   Photochemistry, *J. Geophys. Res.-Atmos.*, *127*(13), doi:10.1029/2022jd036716.

734   Peng, X., T. Wang, W. Wang, A. Ravishankara, C. George, M. Xia, M. Cai, Q. Li, C. M. Salvador, and

735   C. J. Lau (2022), Photodissociation of particulate nitrate as a source of daytime tropospheric Cl_2,

736   *National Science Revew.13*(1), 1-10.

737   Phillips, D. L., R. Inger, S. Bearhop, A. L. Jackson, J. W. Moore, A. C. Parnell, B. X. Semmens, and E.

738   J. Ward (2014), Best practices for use of stable isotope mixing models in food-web studies, *Canadian*

739   *Journal of Zoology*, *92*(10), 823-835, doi:10.1139/cjz-2014-0127.

740   Prabhakar, G., et al. (2017), Observational assessment of the role of nocturnal residual-layer chemistry

741   in determining daytime surface particulate nitrate concentrations, *Atmos Chem Phys*, *17*(23),

742   14747-14770, doi:10.5194/acp-17-14747-2017.

743   Savarino, J., S. Bhattacharya, S. Morin, M. Baroni, and J.-F. Doussin (2008), The NO+ O3 reaction: A

744   triple oxygen isotope perspective on the reaction dynamics and atmospheric implications for the

745   transfer of the ozone isotope anomaly, *The Journal of chemical physics*, *128*(19), 194303.

746   Savarino, J., and M. H. Thiemens (1999), Analytical procedure to determine both $\delta^{18}O$ and $\delta^{17}O$ of

747   H_2O_2 in natural water and first measurements, *Atmos. Environ.*, *33*(22), 3683-3690,

748   doi:https://doi.org/10.1016/S1352-2310(99)00122-3.

749   Savarino, J., W. C. Vicars, M. Legrand, S. Preunkert, B. Jourdain, M. M. Frey, A. Kukui, N. Caillon,

750   and J. Gil Roca (2016), Oxygen isotope mass balance of atmospheric nitrate at Dome C, East

751   Antarctica, during the OPALE campaign, *Atmos. Chem. Phys.*, *16*(4), 2659-2673,

752   doi:10.5194/acp-16-2659-2016.

753   Seinfeld, J. H., and S. N. Pandis (2016), *Atmospheric chemistry and physics: from air pollution to*

754   *climate change*, John Wiley & Sons.

755   Shah, V., et al. (2018), Chemical feedbacks weaken the wintertime response of particulate sulfate and

756   nitrate to emissions reductions over the eastern United States, *Proc. Nat. Acad. Sci. U.S.A.*, *115*(32),

757   8110-8115, doi:10.1073/pnas.1803295115.

758   Slater, E. J., et al. (2020), Elevated levels of OH observed in haze events during wintertime in central

759   Beijing, *Atmos. Chem. Phys.*, 20(23), 14847-14871,

760   Song, W., X.-Y. Liu, Y.-L. Wang, Y.-D. Tong, Z.-P. Bai, and C.-Q. Liu (2020), Nitrogen isotope

761 differences between atmospheric nitrate and corresponding nitrogen oxides: A new constraint using

762 oxygen isotopes, *Sci. Total. Environ.*, *701*, 134515.

763 Stimpfle, R. M., et al. (1999), The coupling of $ClONO_2$, ClO, and NO_2 in the lower stratosphere from

764 in situ observations using the NASA ER-2 aircraft, *J. Geophys. Res.-Atmos.*, *104*(D21), 26705-26714,

765 doi:10.1029/1999jd900288.

766 Su, X., X. Tie, G. Li, J. Cao, R. Huang, T. Feng, X. Long, and R. J. Xu (2017), Effect of hydrolysis of

767 N_2O_5 on nitrate and ammonium formation in Beijing China: WRF-Chem model simulation, *Sci. Total.*

768 *Environ.*, *579*, 221-229.

769 Tan, Z., F. Rohrer, K. Lu, X. Ma, B. Bohn, S. Broch, H. Dong, H. Fuchs, G. I. Gkatzelis, and A.

770 Hofzumahaus (2018), Wintertime photochemistry in Beijing: observations of RO x radical

771 concentrations in the North China Plain during the BEST-ONE campaign, *Atmos. Chem. Phys.*, *18*(16),

772 12391-12411.

773 Tham, Y. J., Z. Wang, Q. Li, W. Wang, X. Wang, K. Lu, N. Ma, C. Yan, S. Kecorius, and A.

774 Wiedensohler (2018), Heterogeneous N_2O_5 uptake coefficient and production yield of $ClNO_2$ in

775 polluted northern China: roles of aerosol water content and chemical composition, *Atmos. Chem. Phys.*,,

776 *18*(17), 13155-13171.

777 Thornton, J. A., et al. (2010), A large atomic chlorine source inferred from mid-continental reactive

778 nitrogen chemistry, *Nature*, *464*(7286), 271-274, doi:10.1038/nature08905.

779 Tørseth, K., W. Aas, K. Breivik, A. M. Fjæraa, M. Fiebig, A.-G. Hjellbrekke, C. Lund Myhre, S.

780 Solberg, and K. E. Yttri (2012), Introduction to the European Monitoring and Evaluation Programme

781 (EMEP) and observed atmospheric composition change during 1972–2009, *Atmos. Chem. Phys.*,,

782 *12*(12), 5447-5481.

783 Vicars, W. C., and J. Savarino (2014), Quantitative constraints on the 17O-excess ($\Delta^{17}O$) signature of

784 surface ozone: Ambient measurements from 50 N to 50 S using the nitrite-coated filter technique,

785 *Geochim. Cosmochim. Acta*, *135*, 270-287.

786 Walters, W. W., and G. Michalski (2015), Theoretical calculation of nitrogen isotope equilibrium

787 exchange fractionation factors for various NOy molecules, *Geochim. Cosmochim. Ac.*, *164*, 284-297.

788 Walters, W. W., and G. Michalski (2016), Theoretical calculation of oxygen equilibrium isotope

789 fractionation factors involving various NO molecules, OH, and H_2O and its implications for isotope

790 variations in atmospheric nitrate, *Geochim. Cosmochim. Acta*, *191*, 89-101,

791 doi:10.1016/j.gca.2016.06.039.

792 Wang, H., X. Chen, K. Lu, Z. Tan, X. Ma, Z. Wu, X. Li, Y. Liu, D. Shang, and Y. Wu (2020),

793 Wintertime N_2O_5 uptake coefficients over the North China Plain, *Science Bulletin*, *65*(9), 765-774.

794 Wang, H., K. Lu, S. Chen, X. Li, L. Zeng, M. Hu, and Y. Zhang (2021), Characterizing nitrate radical

795 budget trends in Beijing during 2013–2019, *Sci. Total. Environ.*, *795*,

796 doi:10.1016/j.scitotenv.2021.148869.

797 Wang, H., K. Lu, X. Chen, Q. Zhu, Z. Wu, Y. Wu, and K. Sun (2018a), Fast particulate nitrate

798 formation via N_2O_5 uptake aloft in winter in Beijing, *Atmos. Chem. Phys.*, *18*(14), 10483-10495,

799 doi:10.5194/acp-18-10483-2018.

800 Wang, H., et al. (2018b), Efficient N_2O_5 uptake and NO_3 oxidation in the outflow of urban Beijing,

801 *Atmos. Chem. Phys.*, *18*(13), 9705-9721, doi:10.5194/acp-18-9705-2018.

802 Wang, H., K. Lu, Z. Tan, X. Chen, Y. Liu, and Y. Zhang (2023), Formation mechanism and control

803 strategy for particulate nitrate in China, J. Environ. Sci., 123, 476-486.

804 Wang, H., K. Lu, Z. Tan, K. Sun, X. Li, M. Hu, M. Shao, L. Zeng, T. Zhu, and Y. Zhang (2017), Model

805   simulation of NO_3, N_2O_5 and $ClNO_2$ at a rural site in Beijing during CAREBeijing-2006, *Atmos. Res.*,

806   *196*, 97-107, doi:10.1016/j.atmosres.2017.06.013.

807   Wang, X., D. J. Jacob, X. Fu, T. Wang, M. L. Breton, M. Hallquist, Z. Liu, E. E. McDuffie, and H. Liao

808   (2020), Effects of Anthropogenic Chlorine on $PM_{2.5}$ and Ozone Air Quality in China, *Environ Sci*

809   *Technol*, *54*(16), 9908-9916, doi:10.1021/acs.est.0c02296.

810   Wang, X., X. Bi, H. Li, W. Zhang, Q. Dai, L. Song, L. Li, J. Wu, Y. Zhang, and Y. Feng (2023), The

811   role of sources and meteorology in driving $PM_{2.5}$-bound chlorine, *Journal of Hazardous Materials*, *441*,

812   129910.

813   Wang, X., H. Wang, L. Xue, T. Wang, L. Wang, R. Gu, W. Wang, Y. J. Tham, Z. Wang, and L. Yang

814   (2017), Observations of N_2O_5 and $ClNO_2$ at a polluted urban surface site in North China: High N_2O_5

815   uptake coefficients and low $ClNO_2$ product yields, *Atmos. Environ.*, *156*, 125-134.

816   Wang, Y. L., W. Song, W. Yang, X. C. Sun, Y. D. Tong, X. M. Wang, C. Q. Liu, Z. P. Bai, and X. Y. Liu

817   (2019), Influences of atmospheric pollution on the contributions of major oxidation pathways to $PM_{2.5}$

818   nitrate formation in Beijing, *J. Geophys. Res-Atmos.*, *124*(7), 4174-4185.

819   Wang, Z., W. Wang, Y. J. Tham, Q. Li, H. Wang, L. Wen, X. Wang, and T. Wang (2017), Fast

820   heterogeneous N_2O_5 uptake and $ClNO_2$ production in power plant and industrial plumes observed in the

821   nocturnal residual layer over the North China Plain, *Atmos. Chem. Phys.*, *17*(20), 12361-12378,

822   doi:10.5194/acp-17-12361-2017.

823   Xia, M., et al. (2020), Significant production of $ClNO_2$ and possible source of Cl_2 from N_2O_5 uptake at

824   a   suburban   site   in   eastern   China,   *Atmos.*   *Chem.*   *Phys.*,   *20*(10),   6147-6158,

825   doi:10.5194/acp-20-6147-2020.

826   Xia, M., et al. (2021), Winter $ClNO_2$ formation in the region of fresh anthropogenic emissions:

827   seasonal variability and insights into daytime peaks in northern China, *Atmos. Chem. Phys.*, *21*(20),

828   15985-16000, doi:10.5194/acp-21-15985-2021.

829   Xia, M., et al. (2019), Heterogeneous Uptake of N_2O_5 in Sand Dust and Urban Aerosols Observed

830   during the Dry Season in Beijing, *Atmosphere*, *10*(4), doi:10.3390/atmos10040204.

831   Xie, X., J. Hu, M. Qin, S. Guo, M. Hu, H. Wang, S. Lou, J. Li, J. Sun, and X. Li (2022), Modeling

832   particulate nitrate in China: current findings and future directions, *Environment International*, 107369.

833   Xue, C., et al. (2020), HONO Budget and Its Role in Nitrate Formation in the Rural North China Plain,

834   *Environ Sci Technol*, *54*(18), 11048-11057, doi:10.1021/acs.est.0c01832.

835   Yan, C., Y. J. Tham, Q. Zha, X. Wang, L. Xue, J. Dai, Z. Wang, and T. Wang (2019), Fast

836   heterogeneous loss of N_2O_5 leads to significant nighttime NOx removal and nitrate aerosol formation at

837   a   coastal   background   environment   of   southern   China,   *Sci.*   *Total.*   *Environ.*,   *677*,   637-647,

838   doi:10.1016/j.scitotenv.2019.04.389.

839   Yang, X., et al. (2022), The impact of chlorine chemistry combined with heterogeneous N_2O_5 reactions

840   on air quality in China, *Atmos. Chem. Phys.*, *22*(6), 3743-3762, doi:10.5194/acp-22-3743-2022.

841   Yu, C., et al. (2020), Heterogeneous N_2O_5 reactions on atmospheric aerosols at four Chinese sites:

842   improving model representation of uptake parameters, *Atmos. Chem. Phys.*, *20*(7), 4367-4378,

843   doi:10.5194/acp-20-4367-2020.

844   Yun, H., T. Wang, W. Wang, Y. J. Tham, Q. Li, Z. Wang, and S. C. N. Poon (2018a), Nighttime NOx

845   loss and $ClNO_2$ formation in the residual layer of a polluted region: Insights from field measurements

846   and an iterative box model, *Sci. Total. Environ*, *622-623*, 727-734, doi:10.1016/j.scitotenv.2017.11.352.

847   Yun, H., W. Wang, T. Wang, M. Xia, C. Yu, Z. Wang, S. C. N. Poon, D. Yue, and Y. Zhou (2018b),

848   Nitrate formation from heterogeneous uptake of dinitrogen pentoxide during a severe winter haze in

849   southern China, *Atmos. Chem. Phys.*, *18*(23), 17515-17527, doi:10.5194/acp-18-17515-2018.

850   Zang, H., et al. (2022), High atmospheric oxidation capacity drives wintertime nitrate pollution in the
851   eastern Yangtze River Delta of China, *Atmos. Chem. Phys.*, *22*(7), 4355-4374,
852   doi:10.5194/acp-22-4355-2022.

853   Zhai, S., et al. (2021), Control of particulate nitrate air pollution in China, *Nat. Geosci.*, *14(6):*
854   *389-395.*, doi:10.1038/s41561-021-00726-z.

855   Zhang, B., H. Shen, X. Yun, Q. Zhong, B. H. Henderson, X. Wang, L. Shi, S. S. Gunthe, L. G. Huey,
856   and S. Tao (2022), Global emissions of hydrogen chloride and particulate chloride from continental
857   sources, *Environmental Science Technology*, *56*(7), 3894-3904.

858   Zhang, Q., et al. (2019), Drivers of improved $PM_{2.5}$ air quality in China from 2013 to 2017,
859   *Proceedings of the National Academy of Sciences*, *116*(49), 24463-24469,
860   doi:10.1073/pnas.1907956116.

861   Zhang, W., et al. (2020), Different HONO Sources for Three Layers at the Urban Area of Beijing,
862   *Environ Sci Technol*, *54*(20), 12870-12880, doi:10.1021/acs.est.0c02146.

863   Zhang, Y.-L., et al. (2022), A diurnal story of $\Delta^{17}O(NO_3^-)$ in urban Nanjing and its implication for
864   nitrate aerosol formation, *npj Climate and Atmospheric Science*, *5*(1),
865   doi:10.1038/s41612-022-00273-3.

866   Zhang, Z., H. Guan, L. Luo, N. Zheng, and H. Xiao (2020), Response of fine aerosol nitrate chemistry
867   to Clean Air Action in winter Beijing: Insights from the oxygen isotope signatures, *Science of The Total*
868   *Environment*, *746*, doi:10.1016/j.scitotenv.2020.141210.

869   Zhang, Z., H. Guan, H. Xiao, Y. Liang, N. Zheng, L. Luo, C. Liu, X. Fang, and H. Xiao (2021a),
870   Oxidation and sources of atmospheric NOx during winter in Beijing based on δ18O-δ15N space of
871   particulate nitrate, *Environ. Pollut.*, *276*, 116708.

872   Zhang, Z., Z. Jiang, H. Guan, Y. Liang, N. Zheng, and W. Guo (2021b), Isotopic evidence for the high
873   contribution of wintertime photochemistry to particulate nitrate formation in Northern China, *J.*
874   *Geophys. Res.-Atmos.*, *126*(22), e2021JD035324.

875   Zhao, X., X. Zhao, P. Liu, D. Chen, C. Zhang, C. Xue, J. Liu, J. Xu, and Y. Mu (2023), Transport
876   Pathways of Nitrate Formed from Nocturnal N_2O_5 Hydrolysis Aloft to the Ground Level in Winter
877   North China Plain, *Environmental Science Technology*, *57*(7), 2715-2725.

878   Zhou, W., et al. (2019), Response of aerosol chemistry to clean air action in Beijing, China: Insights
879   from two-year ACSM measurements and model simulations, *Environ. Pollut.*, *255*,
880   doi:10.1016/j.envpol.2019.113345.

881   Zhou, W., et al. (2018), Production of N_2O_5 and $ClNO_2$ in summer in urban Beijing, China, *Atmos.*
882   *Chem. Phys.*, *18*(16), 11581-11597, doi:10.5194/acp-18-11581-2018.

883

884